Optimal reorientation of geophysical sensors: A quaternion-based analytical solution

Article *in* Geophysics · March 2015

DOI: 10.1190/geo2014-0095.1

2 authors:

Lars Krieger
Institute of Geothermal Resource Management, Bingen (Germany)
35 PUBLICATIONS **239** CITATIONS
SEE PROFILE

Francesco Grigoli
ETH Zurich
39 PUBLICATIONS **379** CITATIONS
SEE PROFILE

GEOPHYSICS, VOL. 80, NO. 2 (MARCH-APRIL 2015); P. 1–12, 7 FIGS., 3 TABLES.
10.1190/GEO2014-0095.1

Optimal reorientation of geophysical sensors: A quaternion-based analytical solution

Lars Krieger[1] and Francesco Grigoli[2]

ABSTRACT

One of the most critical problems affecting geophysical data acquisition procedures is related to the misorientation of multicomponent sensors with respect to a common reference system (e.g., geographic north). In many applications, misoriented sensors affect data analysis procedures, leading to errors in results and interpretations. These problems generally occur in applications where the orientation of the sensor cannot be actively controlled and is not known a priori, e.g., geophysical sensors deployed in borehole installations or on the seafloor. We have developed a quaternion-based method for the optimal reorientation of multicomponent geophysical sensors. In contrast to other approaches, we took into account the full time-series record from all sensor components. Therefore, our method could be applied to all time-series data and was not restricted to a certain type of geophysical sensor. Our method allows the robust calculation of relative reorientations between two-component or three-component sensors. By using a reference sensor in an iterative process, this result can be extended to the estimation of absolute sensor orientations. In addition to finding an optimal solution for a full 3D sensor rotation, we have established a rigorous scheme for the estimation of uncertainties of the resulting orientation parameters. We tested the feasibility and applicability of our method using synthetic data examples for a vertical seismic profile and an ocean bottom seismometer array. We noted that the quaternion-based reorientation method is superior to the standard approach of a single-parameter estimation of rotation angles.

INTRODUCTION

For most geophysical data sets, one tries to achieve the optimal state, in which the sensors are accurately set up so their orientation is known within a very small margin. For many sensor types (e.g., seismometers or magnetotelluric sensors), this local orientation is already referenced to a global reference frame, most commonly geographic or magnetic north. Data obtained from such a set of aligned sensors can be analyzed without additional processing steps (e.g., reorientation), thereby suppressing a potential source of numerical errors. However, in many cases, it is not only likely that the uncertainty of the absolute orientation of the sensors is nonnegligible, but it is just not possible to achieve an accurately determined positioning of the sensors. For instance, we cannot precisely know the orientation of sensors in airborne surveys (see Yun et al., 2008), of geophones within vertical seismic profiles (VSPs), or of free-fall ocean-bottom seismometers (OBSs) and controlled-source electromagnetic sensors (CSEMs) (see Dahm et al., 2002; Myer et al., 2012).

Standard processing schemes for the reorientation of misaligned sensors are often based on an approximative approach under the assumption that the vertical axis orientation is sufficiently close to the correct one, so that any deviation from this can be neglected (e.g., Zeng and McMechan, 2006; Hensch, 2009; Grigoli et al., 2012).

With this approach, the reorientation problem is reduced to a simple rotation in the horizontal plane, leaving the rotation angle as the only parameter to determine. Several methods for the correction of data have been proposed based on this approach. For the analysis of VSP data, these include first the multistep process of pairwise sensor reorientation based on power maximization (DiSiena et al., 1984), polarization analysis (Becquey, 1990; Oye and Ellsworth, 2005), principal component analysis (Michaels, 2001), or crosscorrelation (Zeng and McMechan, 2006). Because these processing

Peer-reviewed code related to this article can be found at http://software.seg.org/2015/0002.
Manuscript received by the Editor 25 February 2014; revised manuscript received 10 July 2014.
[1]University of Adelaide, School of Earth and Environmental Sciences, Adelaide, Australia. E-mail: lars.krieger@adelaide.edu.au.
[2]University of Potsdam, Institute of Earth and Environmental Sciences, Potsdam, Germany. E-mail: francesco.grigoli@geo.uni-potsdam.de.

steps are not linear, a solution cannot be determined by a straight inversion but is obtained through numerical optimization (Hensch, 2009).

For the reorientation of OBS data, one can apply similar methods, for instance, by using artificial reference signals (Nakamura et al., 1987), polarization analysis (Li and Yuan, 1999), or crosscorrelation analysis (Hensch, 2009). In contrast to other methods, the latter example allows us to infer the absolute orientation without further processing by including a land-based reference station into the set of sensors. An analytic single-step solution for relative reorientation of a full data set comprising all sensors at once is described by Grigoli et al. (2012). This method is not restricted to either OBS or VSP data. However, in the latter case, additional processing is required: After reorienting and stacking sensors, a crosscorrelation with a reference signal (Ekström and Busby, 2008) or polarization-analysis-based methods (Jurkevics, 1988) are necessary to determine the absolute orientation.

Although it may be a valid assumption that the vertical component of a geophysical sensor is probably sufficiently well oriented, it is not verifiable. Thus, it remains unclear if this uncertainty really is negligible for all cases. If not, then reorientation consists not only of finding the optimal rotation angle but also the respective rotation axis. Greenhalgh and Mason (1995) discuss the possibility of a VSP sensor that is not vertically oriented. The rotation axis for the reorientation of a three-component sensor can be found by analyzing consecutive parts of a recorded seismic signal. This is possible if the signal source is well determined and the velocity structure of the medium is sufficiently well known in advance (horizontally layered, average velocities known). Another method is presented in Menanno et al. (2013), where the authors analyze first-arrival hodograms of seismic data using a local 3D velocity model. Not many examples for the reorientation of nonseismic sensors can be found, but Key and Lockwood (2010) present a method, working on controlled-source electromagnetic data, in which they simultaneously invert for seafloor conductivity and the respective rotation matrix (using Euler angles). Aside from these approaches, the inclusion of the third component (the vertical one) is usually not considered in reorientation operations.

A basic approach to incorporate the third sensor components is to invert the crosscorrelations between the signals of the three-component sensor and a reference station. Due to the defining integral of the crosscorrelation, there is no possible unique (linear) inversion. An approximate numerical result can be obtained, for instance, by applying multistep optimization methods (e.g., conjugate gradients) with respect to the rotation parameters, or by a sufficiently highly sampled grid search in the space of possible rotations. In the case of a rotation in three dimensions, one has to determine the maximum of $360 \times 180 = 64{,}800$ forward calculated crosscorrelations for a 1° spatial sampling.

We show how to overcome the principal disadvantages of the existing (numerical) solution schemes for the rotational correction in the case of two-component or three-component time-series data. Instead of the calculation of Euler angles, we express rotations using quaternions. This approach had been applied to sets of single pointwise geophysical data before (airborne magnetometric measurements; Yun et al., 2008), but not to sets of continuous time-series data.

We introduce a method for an analytical single-step determination of optimal geophysical sensor reorientation in three dimensions. Unlike other aforementioned approaches, this method uses the full-waveform data of the signal time series; therefore, it is not restricted to the analysis of seismic traces, but it can be applied to all two-component or three-component time-series data. Additionally, it allows us to calculate uncertainties for the estimated reorientation parameters. We present the actual processing scheme and illustrate its application to synthetic data, where we compare the results with a grid-search method.

THEORY

The classical approach to rotations in 3D

A rotation in two dimensions has one degree of freedom and is determined by one scalar value, the rotation angle. Rotations in three dimensions are naturally more complex, have three degrees of freedom, and are usually described via three consecutive rotations about specific basis axes using *Euler angles*. These can be interpreted either in an outer absolute reference frame or in the basis system of the rotated object itself (Euler, 1775; Landau and Lifshitz, 1976). In the latter case, the Euler angles are equivalent to the values of "roll, pitch, and yaw," as they are commonly used in local reference frames of plane or ship movements. If we face the setup of two data sets, one the rotated version of the other, we have to find the respective axes and Euler angles or the equivalent rotation matrix for reorienting the data.

Following algebraic group theory, a composition of rotations is always a rotation itself. Hence, if we express each of the three basic (Euler) rotations using respective 3×3 rotation matrices, we express the effective overall rotation again by a matrix, being the product of the former three. Note that the 3D case is far more complicated than the 2D case. Not only are three spatial axes involved instead of one, but the order of consecutive rotations matters as well because the basic rotations do not commute. This makes it impossible to break down the fundamental problem into subrotations, which could be uniquely described by a set of Euler angles.

Thus, we face the general problem that the overall rotation matrix contains four parameters (three independent), which determine the rotation (axis and the angle) in a nonlinear manner. Therefore, they cannot be determined by a single (linear) inversion of two sets of original and rotated points.

Of course, the solution for this nonlinear problem can be sufficiently approximated by one of two approaches:

1) Forward modeling of rotations using a grid search in all three angles and axes. Depending on the required resolution, this is a numerically demanding process, which is additionally incorporating inherent uncertainties: The rotation matrices hold mainly trigonometric functions, whose accuracy depends on the software and hardware in use.
2) Optimized numerical search algorithms, e.g., steepest descent or conjugate gradients and simplex methods. These yield solutions within a given accuracy and numerical precision. Furthermore, their solutions may represent local minimums in the solution space, and no guarantee can be given that a global optimum solution is returned. Additionally, the computational effort increases with the accuracy because these methods are iterative approaches to a final solution.

In addition to the general issues of nonlinear problems, the classical description of rotations in three dimensions contains another possible pitfall. Due to the periodicity of the trigonometric

functions and the generally orthogonal reference system of the Euler angles, specific configurations of the Euler angle triple exist, in which the basis axes are no longer independent (combinations of $0, \pi/2, \pi$). In these cases, the chosen system of angles and basis axes is no longer sufficient to uniquely describe the current state of the system; this is known as *gimbal lock* (see Brezov et al., 2013). Because real data sets are handled numerically, this state can be reached if the angle values are numerically close to such a critical triple. The potential occurrence of a gimbal lock is another source of uncertainty in the numerical results.

Rotations in three dimensions using quaternions

To overcome the potential sources of errors mentioned in the previous section, we have to change the way of describing rotations in three dimensions. It turns out that by using quaternions, many of these problems can be circumvented.

The application of quaternions is not a new development, but it is not yet widely used within the geosciences. Geophysical applications include the deconvolution of multicomponent seismic traces (Menanno and Mazzotti, 2012), time-lapse analysis of image data sets (Witten and Shragge, 2006), multicomponent seismic velocity analysis (Grandi et al., 2007), rotation parameter inversion in orthorhombic media (Lapilli and Fowler, 2014), and the analysis of double-couple earthquake sources (Kagan, 1991; Cesca et al., 2014). The basic properties of quaternions that are important for the determination of the rotations in three dimensions are briefly described in the following paragraphs.

Properties of quaternions

The space $\mathbb{H}$ of quaternions forms a division algebra over $\mathbb{R}^4$, which was introduced by Hamilton (1853). Due to the isomorphism $\mathbb{H} \simeq \mathbb{R}^4$, elements $\mathbf{q}$ of the quaternion field $\mathbb{H}$ may be interpreted as elements of a 4D real vector space. We interpret $\mathbb{H} \simeq \mathbb{R} \times \mathbb{R}^3$; hence, a quaternion $\mathbf{q}$ can be written as a combination of a scalar (*real*) and a vector (*imaginary*) part:

$$\mathbf{q} = (q_0, [q_1, q_2, q_3]) =: (s_{\mathbf{q}}, \mathbf{v}_{\mathbf{q}}) \in \mathbb{R} \times \mathbb{R}^3. \tag{1}$$

We can identify the $\mathbb{R}^3$ with the subspace ${}^i\mathbb{H} \subset \mathbb{H}$ of vanishing real parts

$$\mathbb{R}^3 \simeq {}^i\mathbb{H} := \{\mathbf{q} | s_{\mathbf{q}} = 0, \mathbf{v}_{\mathbf{q}} \in \mathbb{R}^3\}. \tag{2}$$

Equation 2 allows the mapping of a 3D real vector uniquely onto an element of the quaternion algebra:

$$\mathbb{R}^3 \to {}^i\mathbb{H}, \qquad \mathbf{x} \mapsto \underset{\sim}{\mathbf{q}}_{\mathbf{x}}. \tag{3}$$

The quaternion addition and scalar multiplication are defined componentwise. Additionally, there is a pairwise quaternion product $\otimes$:

$$\mathbf{q} \otimes \mathbf{p} := (s_{\mathbf{p}} \cdot s_{\mathbf{q}} - \mathbf{v}_{\mathbf{q}} \cdot \mathbf{v}_{\mathbf{p}}, s_{\mathbf{p}} \cdot \mathbf{v}_{\mathbf{q}} + s_{\mathbf{q}} \cdot \mathbf{v}_{\mathbf{p}} + \mathbf{v}_{\mathbf{p}} \times \mathbf{v}_{\mathbf{q}}), \tag{4}$$

with the inner product "$\cdot$" as well as the standard outer 3D vector crossproduct "$\times$." The product is associative, but in general not commutative.

Rotations in 3D

Consider a rotation that transforms $\mathbf{x}$ into $\mathbf{x}'$ ($\mathbf{x}, \mathbf{x}' \in \mathbb{R}^3$). This operation is defined by the rotation angle $\alpha \in [0°, 360°[$ and a unit vector $\hat{\boldsymbol{\rho}} \in \mathbb{R}^3$ in the direction of the rotation axis. To express the rotation in terms of quaternions, we first use the isomorphism in equation 2 for defining the equivalent quaternions $\underset{\sim}{\mathbf{x}} = (0, \mathbf{x})$ and $\underset{\sim}{\mathbf{x}}' = (0, \mathbf{x}')$.

We know, for instance, from Horn (1987), that there is a unit quaternion $\hat{\underset{\sim}{\mathbf{q}}}$ ("rotation quaternion") with an involution $\bar{\hat{\underset{\sim}{\mathbf{q}}}}$ (equivalent to the complex conjugation in $\mathbb{C}$) so that

$$\underset{\sim}{\mathbf{x}}' = \hat{\underset{\sim}{\mathbf{q}}} \otimes \underset{\sim}{\mathbf{x}} \otimes \bar{\hat{\underset{\sim}{\mathbf{q}}}}. \tag{5}$$

This means that we can express a rotation in three dimensions using a quaternion product. The quaternion, which describes a rotation of an angle α about an axis $\hat{\boldsymbol{\rho}}$ is given by the normalization of

$$\underset{\sim}{\mathbf{q}} = \left(\cos\frac{\alpha}{2}, \sin\frac{\alpha}{2} \cdot \hat{\boldsymbol{\rho}}\right). \tag{6}$$

The three degrees of freedom of the rotation in three dimensions are incorporated in the four free components of the quaternion together with the constraint of the normalization.

From the definition of the quaternion multiplication, we see

$$-\hat{\underset{\sim}{\mathbf{q}}} \otimes \underset{\sim}{\mathbf{x}} \otimes -\bar{\hat{\underset{\sim}{\mathbf{q}}}} = \hat{\underset{\sim}{\mathbf{q}}} \otimes \underset{\sim}{\mathbf{x}} \otimes \bar{\hat{\underset{\sim}{\mathbf{q}}}}. \tag{7}$$

Thus, we are free in the choice of sign for the rotation quaternion.

The concatenation of two rotations transforms $\mathbf{x}$ via $\mathbf{x}'$ into $\mathbf{x}''$. We express these rotations using the unit quaternions $\hat{\underset{\sim}{\mathbf{q}}}$, $\hat{\underset{\sim}{\mathbf{p}}}$:

$$\begin{aligned} \underset{\sim}{\mathbf{x}}'' &= \hat{\underset{\sim}{\mathbf{p}}} \otimes \underset{\sim}{\mathbf{x}}' \otimes \bar{\hat{\underset{\sim}{\mathbf{p}}}} = \hat{\underset{\sim}{\mathbf{p}}} \otimes (\hat{\underset{\sim}{\mathbf{q}}} \otimes \underset{\sim}{\mathbf{x}} \otimes \bar{\hat{\underset{\sim}{\mathbf{q}}}}) \otimes \bar{\hat{\underset{\sim}{\mathbf{p}}}} \\ &= (\hat{\underset{\sim}{\mathbf{p}}} \otimes \hat{\underset{\sim}{\mathbf{q}}}) \otimes \underset{\sim}{\mathbf{x}} \otimes (\bar{\hat{\underset{\sim}{\mathbf{p}}}} \otimes \bar{\hat{\underset{\sim}{\mathbf{q}}}}) =: \hat{\underset{\sim}{\mathbf{pq}}} \otimes \underset{\sim}{\mathbf{x}} \otimes \bar{\hat{\underset{\sim}{\mathbf{pq}}}}. \end{aligned} \tag{8}$$

Hence, combined rotations are again expressed by only one rotation quaternion $\hat{\underset{\sim}{\mathbf{pq}}}$, which is obtained from (left-sided) multiplications of the respective successive rotation quaternions.

Data

Unlike other reorientation methods (e.g., Menanno et al., 2013), we do not need to restrict the analysis to certain features in the signal, e.g., specific phases in seismic traces. Therefore, our method is applicable to the general class of multicomponent time-series data, for instance, magnetic field measurements.

We consider orthogonal three-component data sets. For the handling of two-component data, they are extended by adding a third zero-valued component in a first processing step. The time-series data for each component are finitely sampled and of finite length L. If $\mathbf{p}(t)$ are the original and $\mathbf{r}(t)$ the rotated data, we have two points $(p_1, p_2, p_3), (r_1, r_2, r_3) \in \mathbb{R}^3$ for each point in time t_l. The time series are therefore equivalent to sets of points $\{\mathbf{p}_t\}$, $\{\mathbf{r}_t\}$ ($|\{\mathbf{p}_t\}| = |\{\mathbf{r}_t\}| = L$).

The coordinates of the points from both sets are transformed into relative coordinates by correcting for the respective center of mass:

$$\{\mathbf{p}_t\} \mapsto \{\mathbf{p}_t{}'\}; \qquad \{\mathbf{r}_t\} \mapsto \{\mathbf{r}_t{}'\}. \tag{9}$$

All coordinates from here on are assumed to be given in this reference frame, so we omit the prime for readability.

One can find a rotation operator, which, applied onto set $\{\mathbf{p}_t\}$, minimizes the deviation from $\{\mathbf{r}_t\}$. To calculate this deviation, we have to define a suitable norm for time-series data of length L for single components d:

$$\|d\|^2 = \sum_{i=1}^{L} d(t_i)^2, \tag{10}$$

and in extension of this for three-component data $\mathbf{D} = (D_1, D_2, D_3)$:

$$\|\mathbf{D}\|^2 = \sum_{i=1}^{L} D_1(t_i)^2 + D_2(t_i)^2 + D_3(t_i)^2. \tag{11}$$

With $\Delta_{\mathbf{p_1},\mathbf{p_2}} := \mathbf{p_2} - \mathbf{p_1}$ as the absolute data deviation between two data sets $\mathbf{p_1}(t)$ and $\mathbf{p_2}(t)$, we express the normalized overall deviation as the percentage *residual "Res"*:

$$\mathrm{Res} := \frac{\|\Delta_{\mathbf{p_1},\mathbf{p_2}}\|}{\|\mathbf{p_1}\|} \cdot 100. \tag{12}$$

Estimation of the optimal rotation between two data sets

The reorientation of three-component time-series data sets is equivalent to the following problem: Given the two sets of points in the 3D space $\{\mathbf{p}_t\}, \{\mathbf{r}_t\}$, we are interested in finding the optimal rotation operator that transforms $\{\mathbf{p}_t\}$ into $\{\mathbf{r}_t\}$. The solution can be found in publications on the theory of quaternions; for instance, in Horn (1987). In the following, we show only the main steps to obtain the least-squares optimized estimation of the reorientation.

First, we collect the sum $\mathbf{S}$ of outer products of the original $\mathbf{p}(t_l)$ and rotated $\mathbf{r}(t_l)$ position vectors of the lth data point (sample on the time axis):

$$\mathbf{S} := \sum_{l=1}^{L} {}^{l}\mathbf{p} \cdot {}^{l}\mathbf{r}^T = \begin{pmatrix} S_{11} & S_{12} & S_{13} \\ S_{21} & S_{22} & S_{23} \\ S_{31} & S_{32} & S_{33} \end{pmatrix}. \tag{13}$$

From the entries of $\mathbf{S}$, we build the real valued symmetric matrix $\mathbf{N}$:

$$\mathbf{N} = \begin{pmatrix} S_{11}+S_{22}+S_{33} & S_{23}-S_{32} & S_{31}-S_{13} & S_{12}-S_{21} \\ S_{23}-S_{32} & S_{11}-S_{22}-S_{33} & S_{12}+S_{21} & S_{31}+S_{13} \\ S_{31}-S_{13} & S_{12}+S_{21} & -S_{11}+S_{22}-S_{33} & S_{23}+S_{32} \\ S_{12}-S_{21} & S_{31}+S_{13} & S_{23}+S_{32} & -S_{11}-S_{22}+S_{33} \end{pmatrix}. \tag{14}$$

The optimal rotation between the two given data sets can be expressed by a single unit quaternion. This quaternion is given by the normalized eigenvector of $\mathbf{N}$, which belongs to $\mathbf{N}$'s largest eigenvalue:

$$\underset{\sim}{\hat{\mathbf{q}}}_{\mathrm{opt}} = \frac{\underset{\sim}{\boldsymbol{\nu}_1}}{\|\underset{\sim}{\boldsymbol{\nu}_1}\|}, \quad \mathbf{N} \cdot \boldsymbol{\nu}_\mathbf{i} = \lambda_i \cdot \boldsymbol{\nu}_\mathbf{i}, \quad i \in \{1, \ldots, 4\}, \tag{15}$$

where $\lambda_1 \geq \lambda_2 \geq \lambda_3 \geq \lambda_4$. Hence, the underlying rotation between the two data sets can be expressed by

$${}^{l}\underset{\sim}{\mathbf{r}} \approx \underset{\sim}{\hat{\mathbf{q}}}_{\mathrm{opt}} \otimes {}^{l}\underset{\sim}{\mathbf{p}} \otimes \underset{\sim}{\bar{\hat{\mathbf{q}}}}_{\mathrm{opt}} \quad \forall\, l \in [1, L]. \tag{16}$$

This again is equivalent to a rotation about the estimated rotation axis $\boldsymbol{\rho} = \boldsymbol{\rho}(\underset{\sim}{\hat{\mathbf{q}}}_{\mathrm{opt}})$ by the angle $\alpha = \alpha(\underset{\sim}{\hat{\mathbf{q}}}_{\mathrm{opt}})$. Both quantities, axis and angle, can be obtained from the calculated unit quaternion $\boldsymbol{\nu}_1$.

The eigenvalues of $\mathbf{N}$ can be nondistinct if sets $\{\mathbf{p}\}$ and $\{\tilde{\mathbf{r}}\}$ are each perfectly located on respective colinear coordinates. In this case, the described algorithm yields nonunique rotation parameters. This setup can be neglected for all practical purposes; hence, we assume distinct eigenvalues for $\mathbf{N}$ for the remainder of this work.

Estimation of uncertainties

The rotation of a point in $\mathbb{R}^3$ is not necessarily a continuous function with respect to the entries of the rotation matrix, but the rotation expressed by quaternions is continuous. This allows not only a linear interpolation between two rotated states but also a straight forward error calculation.

In contrast to the implementation of other methods (e.g., Grigoli et al., 2012), the quaternion approach allows a direct estimation of uncertainties of the rotation axis and angle. They are determined by eigenvalues and eigenvectors of the matrix $\mathbf{N}$. Thus, we are interested in the influence of noise on the respective variables.

Uncertainty of the largest eigenvalue λ_1

Let $\mathbf{V}$ be the matrix that contains the four normalized (column) eigenvectors of $\mathbf{N}$:

$$\mathbf{V} := (\boldsymbol{\nu}_1, \boldsymbol{\nu}_2, \boldsymbol{\nu}_3, \boldsymbol{\nu}_4). \tag{17}$$

Because $\mathbf{N}$ is real and symmetric, we know that $\mathbf{V}$ is orthogonal. The eigenvectors of the perturbed matrix $\mathbf{N} + \delta\mathbf{N}$ are given as $\boldsymbol{\mu}_\mathbf{i}$. Bauer and Fike's (1960) theorem now yields a relation between the eigenvalues of the original and the perturbed matrix, respectively:

$$|\boldsymbol{\nu}_\mathbf{i} - \boldsymbol{\mu}_\mathbf{i}| \leq \kappa(\mathbf{V}) \cdot \|\delta\mathbf{N}\| \qquad i \in \{1, \ldots, 4\}, \tag{18}$$

where κ is the condition number. Because $\mathbf{V}$ is orthogonal, we have $\kappa(\mathbf{V}) = 1$. Thus, the deviation of the eigenvalues is bounded by the norm of the uncertainty matrix. Therefore, the determination of the largest eigenvalue of $\mathbf{N}$ will be unique for reasonably small uncertainties on the data.

Uncertainty of the eigenvector $\boldsymbol{\nu}_1$

From perturbation theory (e.g., Schrödinger, 1926), we obtain an estimation for the deviation $\delta\boldsymbol{\nu}_1$ from the eigenvector $\boldsymbol{\nu}_1$ of $\mathbf{N}$, caused by the error matrix $\delta\mathbf{N}$:

$$\delta\boldsymbol{\nu}_1 = \sum_{j=2}^{4} \frac{\boldsymbol{\nu}_\mathbf{j}^T \cdot \delta\mathbf{N} \cdot \boldsymbol{\nu}_1}{\lambda_1 - \lambda_j} \boldsymbol{\nu}_\mathbf{j}. \tag{19}$$

This represents the cumulative effect of the deviations from the orthogonal relationship between the eigenvectors, caused by the error matrix. The deviations are weighted with regard to the difference of the respective eigenvalues, so eigenvectors with small eigenvalues have only a small influence, even if they are perturbed in a significantly nonorthogonal direction.

As shown earlier in equation 6, the first component of $\boldsymbol{\nu_1}$ determines the rotation angle and the other three stand for the rotation axis orientation. Hence, it is not advisable to state just an overall uncertainty percentage in terms of a deviation vector norm. The two quantities *angle* and *axis* should be interpreted independently, yielding an absolute uncertainty of the rotation angle $\delta\alpha$ and an opening angle ε of a cone around the determined rotation axis, respectively (see Figure 1). Therefore, we derive two quaternions $\underset{\sim}{\boldsymbol{\nu}}_{\mathbf{1}}^{\text{upper}}$ and $\underset{\sim}{\boldsymbol{\nu}}_{\mathbf{1}}^{\text{upper}}$ as the lower and upper bounds for the uncertainty from the perturbed eigenvector:

$$\underset{\sim}{\boldsymbol{\nu}}_{\mathbf{1}}^{\text{upper}} := \boldsymbol{\nu_1} - \delta\boldsymbol{\nu_1}; \qquad \underset{\sim}{\boldsymbol{\nu}}_{\mathbf{1}}^{\text{upper}} := \boldsymbol{\nu_1} + \delta\boldsymbol{\nu_1}. \tag{20}$$

From these bounds, we use a conservative approach to estimate the uncertainty $\delta\alpha$ of the rotation angle α:

$$\delta\alpha = \max_{g\in[\text{upper,lower}]} |\alpha(\underset{\sim}{\boldsymbol{\nu}}_{\mathbf{1}}^{g}) - \alpha(\boldsymbol{\nu_1})|, \tag{21}$$

and the uncertainty of the rotation axis $\boldsymbol{\rho}$ by finding the maximum deviation of the rotation axis. This is determined by calculating the maximum opening angle ε of a cone around $\boldsymbol{\rho}$. With $\angle(\mathbf{a},\mathbf{b})$ as the opening angle between two vectors in $\mathbb{R}^3$, we obtain

$$\varepsilon = \max_{g\in[\text{upper,lower}]} \angle(\boldsymbol{\rho}(\boldsymbol{\nu}_{\mathbf{1}}^{g}), \boldsymbol{\rho}(\boldsymbol{\nu_1})). \tag{22}$$

Estimation of $\delta\mathbf{N}$

The estimation of the uncertainties is based on the eigenvalues and eigenvectors of the matrix $\mathbf{N}$ from optimal, unperturbed data (see equation 19). However, this matrix will not be known from observed data. To overcome this problem, we have to assume that $\mathbf{N}$ can be sufficiently well approximated with the respective matrix $\bar{\mathbf{N}}$ calculated from observed data:

$$|\bar{\mathbf{N}} - \mathbf{N}| \le \delta\mathbf{N}, \tag{23}$$

so that the eigenvalues and eigenvectors of $\bar{\mathbf{N}}$ can be used for the estimation of $\delta\nu_1$.

The determination of the actual uncertainty matrix $\delta\mathbf{N}$ may vary for different data sets, for instance, due to the incorporation of known systematic errors. However, for many cases, it is a reasonable approach to assume that the noise is independently distributed and the noise level σ_{p_m} (σ_{r_m}) is constant for each component $m \in \{1,2,3\}$. Then Gauss' standard expression for the propagation of errors is a valid approximation. Under these assumptions, we obtain the entries of $\delta\mathbf{N}$ by calculating

$$S_{mn} = \sum_{l=1}^{L} {}^{l}p_m \cdot {}^{l}r_n; \qquad m,n \in \{1,2,3\}, \tag{24}$$

$$\sigma_{S_{mn}} = \sqrt{\sigma_{p_n}^2 \cdot \sum_{l=1}^{L} {}^{l}r_m^2 + \sigma_{r_m}^2 \cdot \sum_{l=1}^{L} {}^{l}p_n^2}, \tag{25}$$

and finally combining the $\sigma_{S_{kl}}$ for each component $\delta\mathbf{N}_{ij}$ accordingly.

In cases in which the noise level can be assumed to be the same for all components, the latter expression can be simplified:

$$\sigma_0 := \sigma_{p_m} = \sigma_{r_m} \quad \forall\ m,n \in \{1,2.3\}, \tag{26}$$

$$\sigma_{S_{mn}} = \sigma_0 \cdot \sqrt{\sum_{l=1}^{L} {}^{l}r_m^2 + {}^{l}p_n^2}. \tag{27}$$

APPLICATIONS

General considerations

The method presented here aims to find the optimal rotation between two arbitrary 3D data series. To apply the scheme to a geophysical data set, a few points have to be considered:

- The data have to be given in an orthogonal coordinate system. If the sensors had not been positioned appropriately, this has to be corrected for.
- Our approach demands a sufficient similarity of the measured signals. To ensure that this criterion is satisfied, the spatial sensor separation d must be small compared with the main signal wavelength $d \ll \lambda$. To achieve this, data have to be frequency low-pass filtered in advance of further processing. This again is a standard procedure, applied in most reorientation methods.
- Because we are only interested in the optimal rotation between two data sets, other influences on the differences between the data sets must be suppressed. Therefore, as a second step, the time lag caused by finite distances between sensors is removed by standard crosscorrelation optimization or using beam forming methods.
- The rotation using quaternions is carried out in three spatial dimensions, allowing three degrees of freedom: three components of the rotation axis and one rotation angle, together under the constraint of being expressed by a unit vector. This number cannot be systematically restricted, so two-component data sets must be extended by adding a third vertical (zero) component. This then results in a rotation about the

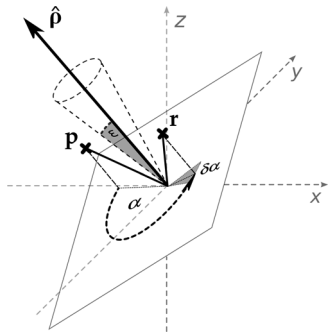

Figure 1. Geometrical interpretation of the uncertainties for a rotation operation between the points $\mathbf{p}$ and $\mathbf{r}$. The real and imaginary parts of the uncertainty $\delta\boldsymbol{\nu_1}$ of the resulting eigenvector of $\mathbf{N}$ yield the uncertainty $\delta\alpha$ of the rotation angle α and the deviation of the rotation axis $\hat{\boldsymbol{\rho}}$, expressed by the opening angle ε of the uncertainty cone around the axis.

vertical axis. However, the resulting uncertainties will still be distributed between the rotation angle and the axis, which potentially allows a deviation of the effective rotation axis from the normal vector of the surface defined by the 2D data set. This effect must be taken into account for a correct interpretation of the result.

- The optimal quaternion rotation is based on relative coordinates. This means that the center of mass of all components' data must be at zero, which is equivalent to a demeaning of all traces as a third processing step. For a comparison of a reoriented data set with another reference set, the respective mean values of the components must be adjusted.
- The respective optimal rotation quaternion is found between pairs of sensors. In the case of several sensors to be reorientated, one sensor takes the role of a reference sensor. In cases in which the deviations between the signals of the sensors increase strongly with distance from the reference sensor, it is more suitable to calculate the reorientations between adjacent sensors. Beginning with the reference sensor, consecutive pairwise processing of neighboring sensors then yields a set of quaternions. These calculations are mutually independent; hence, they can be parallelized to reduce the computational time of this processing step. Applying the (left-sided) quaternion product to the resulting quaternions allows for a one-step correction of each sensor with respect to the reference.
- Eigenvectors for the matrices are calculated numerically. Depending on the implementation of this process, the uncertainties may vary. For the calculation of the results presented in this publication, we used the routines of the Numpy and Scipy modules of Python. Bootstrap tests for random 4×4 matrices show that these numerical errors are negligible compared to the influence of any of the uncertainties of the data.
- Data sets or just single components may have gaps, but only sections of data with full information from all components can be used for the reorientation of the sensors.

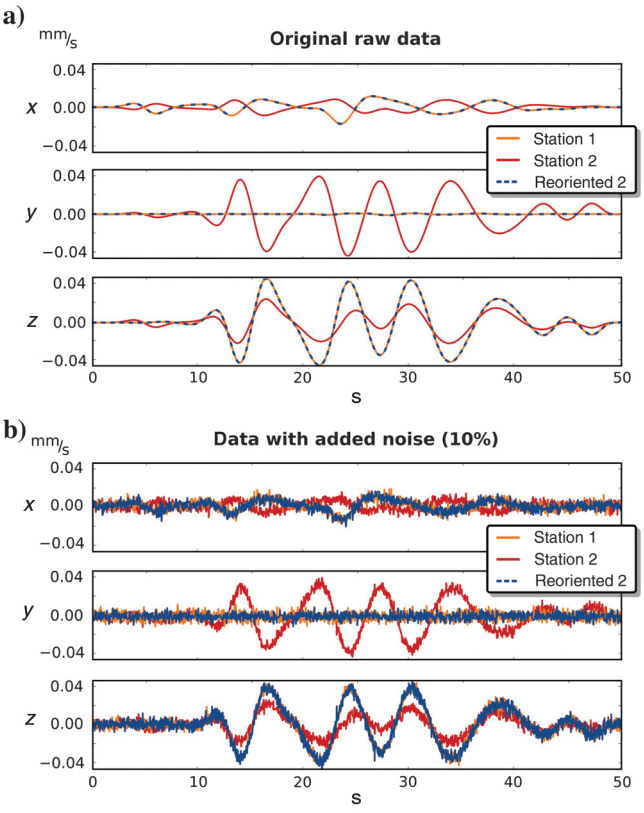

Figure 2. Example of rotated synthetic data: (a) Raw data. (b) Data with added noise. The orientation of station 2 (red) is rotated by 131° about the axis (24.2, −54.3, 80.4) with respect to station 1 (orange). The result from the estimated optimal reorientation of station 2 data is shown in blue (dotted line). The estimation coincides with the correct values in case of raw data (a). For data with added noise (b) the values deviate from the correct rotation by 0.7° in the orientation of the axis and 0.8° in the rotation angle. (see Table 1)

The first steps are essential parts of standard data processing schemes, and they can be handled independently from the rotation problem in various ways. This work focuses on the methodology of finding the optimal solution for the sensor reorientation problem, including an analytical error estimation. Here, we demonstrate the principal applicability of the method by two examples of synthetic data sets. We assume that the aforementioned properties hold for all example sets: The data are complete, sufficiently frequency low-pass filtered, and corrected for time lags.

Three-component data — Proof of concept under optimal conditions

As a proof of concept, we consider an optimized case: The original data traces for all sensors are identical. We use a three-component synthetic velocity seismogram of 50-s length and a sampling rate of 50 Hz. We take the low-pass frequency-filtered data from station 1 from Figure 4 (see Figure 2a for a detailed visualization of the original data). This seismogram is assigned to six different sensors (stations 1–6). Because the data are identical, this does not resemble a realistic geometry, but it is rather a set of six independent rotation examples. The orientations of sensors 2–6 are altered randomly, and the quaternion algorithm is used to estimate the optimal reorientation.

In the absence of noise, this process yields a perfect match between the original data and the rerotated sets (Figure 2a). In a second step, we add random noise to the data components after the rotation. The noise is obtained from a standard random number generator, using a normal distribution and 10% of the maximum data amplitude as its σ value. This level of white noise is not realistic for already low-pass frequency-filtered time-series data. We apply this level of noise to demonstrate the robustness of the algorithm, which is implicitly based on the samplewise comparison of the respective components of the original and the rotated data. The reorientation is calculated for the data set with added noise. A data example is shown in Figure 2b.

The reorientation parameters are calculated together with the estimates for the uncertainties ϵ and $\delta\alpha$. In this setup, we have information about both matrices $\bar{\mathbf{N}}$, calculated from the "observed" (noisy) data, and $\mathbf{N}$, calculated from the original (noise-free) data set. So we can compare the uncertainties, independently derived from those matrices. It turns out that the actual variations of rotation axis and angle are systematically underestimated by the uncertainties calculated from the eigenvalues and eigenvectors of the unperturbed matrix $\mathbf{N}$. However, they all lie within the uncertainty

boundaries derived from $\bar{\mathbf{N}}$. This indicates that it is possible to infer uncertainties of the calculated reorientation parameters directly from the estimated mean overall noise level of the observed data. However, a detailed study of how the occurrence of various noise characteristics in the data (systematic and random) influences the parameter estimation is beyond the scope of this paper.

The numerical results of the reorientation are given in Table 1. The level of the residual value Res depends only on the absolute level of the noise added to the data. It does not contain significant information on the error of the calculated reorientation parameters.

Three-component data — A vertical seismic profile geometry

We have shown that the quaternion algorithm works on optimal data, and we have determined the influences of random noise on the result of the reorientation. The latter application can be interpreted as an approximation of a small-aperture seismic array, where the distance between stations are in the order of a few hundred meters, negligible with respect to the distance of the source. The frequency-filtered recorded waveforms show a very high degree of similarity, so they can be considered almost identical. However, we now consider the realistic survey geometry of a VSP. Within the VSP, six sensors are vertically aligned, but the relative orientation of the sensors is unknown. The velocity model is a one-dimensionally layered half-space, and the geometry is shown in Figure 3. We use the E3D code described by Larsen and Grieger (1998) to calculate synthetic seismograms for an arbitrarily chosen source mechanism (explosion).

The original data are set up so that the intersensor distances are negligible compared to the signal main wavelengths. The data from neighboring sensors show a degree of similarity, which allows a direct application of reorientation without further processing (see Figure 4a). However, in this section, we also want to demonstrate the influence of frequency filtering the data. Therefore, we generate a second data set by applying a zero-phase Butterworth low-pass

Table 1. Quaternion method parameter estimates, including uncertainties for the reorientation of optimal data with added noise (10%). Here, N is calculated from the original (noise-free) data, and $\bar{\mathbf{N}}$ is calculated from the noisy data; $\angle\hat{\rho}$ denotes the deviation from the axis $\hat{\rho}$; and angles ϵ, α, $\delta\alpha$, and $\angle\hat{\rho}$ are given in degrees.

	Forward rotation		Reorientation					N		$\bar{\mathbf{N}}$	
Station	$\hat{\rho}$	α	$\hat{\rho}$	$\angle\hat{\rho}$	α	$\Delta\alpha$	Res	ϵ	$\delta\alpha$	ϵ	$\delta\alpha$
Sta 1	—	—	—	—	—	—	—	—	—	—	—
Sta 2	(24.2, −54.3, 80.4)	131	(25.4, −54.2, 80.1)	0.7	130.2	0.8	48.7	0.60	0.73	1.43	0.90
Sta 3	(26.1, 50.8, 82.1)	14	(27.0, 50.8, 81.8)	0.6	12.8	1.2	49.0	0.43	1.01	1.09	1.33
Sta 4	(28.6, 23.0, 93.0)	−6	(19.4, 22.8, 95.4)	5.5	−8.1	2.1	48.8	8.94	1.69	19.20	2.27
Sta 5	(−65.8, 73.2, 17.8)	−42	(−65.4, 72.6, 21.4)	2.1	−42.4	0.4	49.0	1.84	0.34	4.67	0.44
Sta 6	(68.7, −47.3, 55.2)	−135	(69.1, −45.9, 55.8)	0.9	−135.5	0.5	48.5	0.80	0.48	1.86	0.58

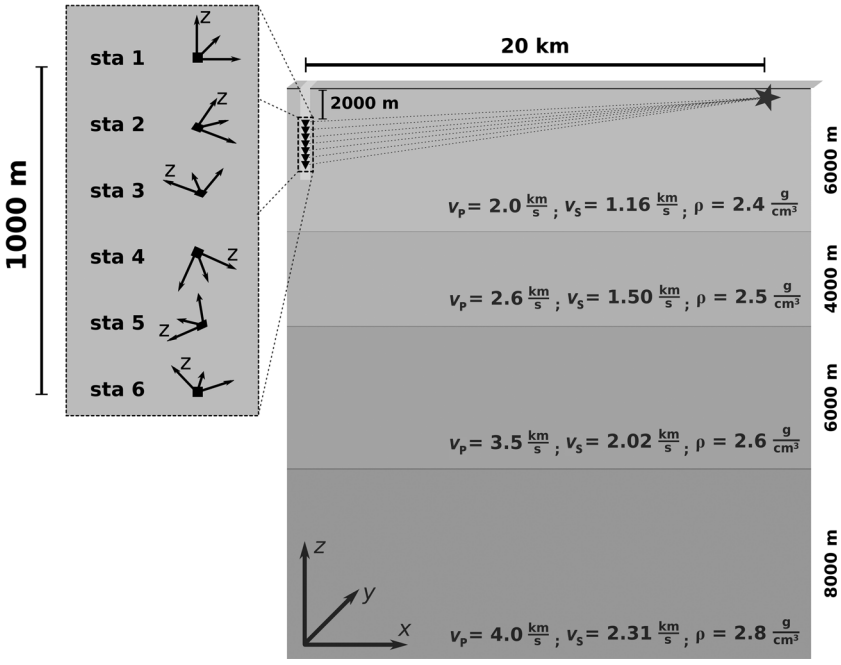

Figure 3. VSP geometry and earth velocity model for the generation of synthetic seismograms using E3D (Larsen and Grieger, 1998). The (explosive) source location is marked by a star, and the idealized direct signal raypath sketches are indicated by dotted lines. The model is continued by a half-space underneath the shown layers. The schematic receiver geometry is shown in the enlarged section.

frequency filter of order 4 with a corner frequency of 0.1 Hz, including renormalization, to the original data set (using ObSpy; Beyreuther et al., 2010). See Figure 4b for a visualization of all respective data components.

The data of stations 2–6 are again rotated with randomly chosen angles and axes, and we carry out the reorientation of stations 2–6 with respect to the topmost station 1 for both data sets: the original and the low-pass filtered. Examples of the resulting reoriented data (original and low-pass frequency filtered) are shown in Figure 5.

Before we estimate the rotation, we take into account possible time lags of the signal between different sensors. First, we normalize the data to correct for potential geometry damping of the signal, and second, we calculate the crosscorrelation between the signal energy of the stations. This yields the optimal shift in time for the data of each station. Throughout our tests with the given data sets, the resulting time shifts are very small ($\lesssim$0.04 s).

The results of the reorientation of the two data sets show that the estimation of rotation parameters works for a realistic setup of nonidentical data. The numerical values for both data sets are consistent, but show variations. Numerical values for a realization example can be found in Table 2. In most cases, the rotation parameters determined from the low-pass filtered data were closer to the correct values than the ones derived from the original unfiltered data. The residual Res is always lower for the low-pass-filtered data. We also generated another data set from low-pass frequency filtering with an even lower corner frequency. It turned out that the parameters estimated with that set are consistently worse than the values obtained from the unfiltered data.

We calculated the uncertainty estimates $\delta\alpha$ and ϵ by using a matrix $\delta\mathbf{N}$, which was calculated from the difference between the matrices $\mathbf{N}_{\text{original}}$ and $\mathbf{N}_{\text{filtered}}$. Then, we obtained two sets $\{\delta\alpha_{\text{original}}, \delta\alpha_{\text{filtered}}\}$, $\{\epsilon_{\text{original}}, \epsilon_{\text{filtered}}\}$ by using the respective eigenvectors and eigenvalues. We observed that in most cases, the uncertainties $\delta\alpha$ derived from the low-pass filtered data are larger than from the original data and vice versa for the values of ϵ. When taking the maximum uncertainty in each case, these are good bounds for the actual errors of the estimated rotation and axis angles.

We also analyzed of the influence of added noise in both data sets, which showed that the effect of noise as described in the former section can be considered as purely additive. The increase of the residuals Res and the values for the uncertainties $\delta\alpha$ and ϵ increased as derived before. Therefore, we do not include numerical results here.

The two data sets show large similarities between data from neighboring sensors, so they are both well suited to be used for

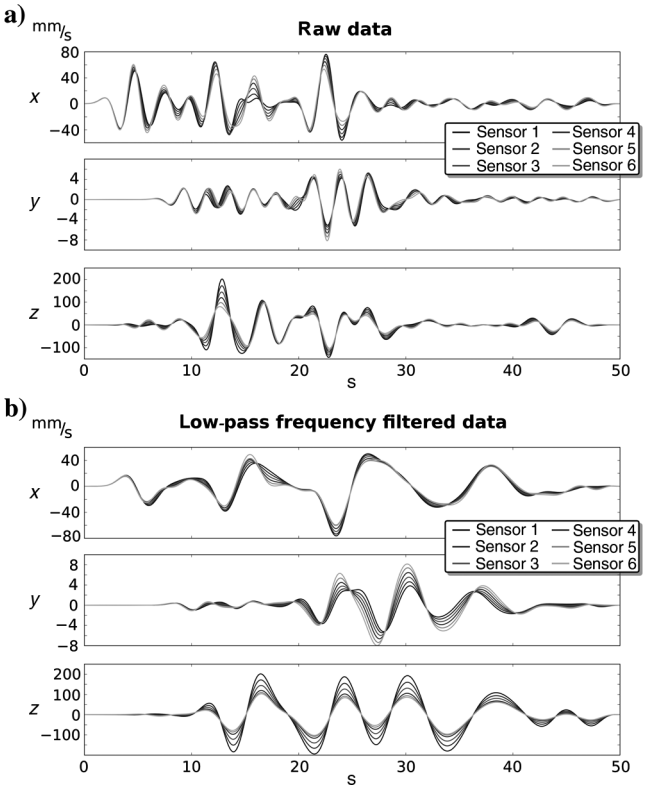

Figure 4. Synthetic data for the geometry shown in Figure 3. The stations are enumerated with increasing distance from the source location. (a) Raw synthetic seismograms. (b) Low-pass frequency filtered data. The filter is a zero-phase Butterworth low-pass of order 4 with a corner frequency of 0.1 Hz (calculated using ObSpy; Beyreuther et al., 2010).

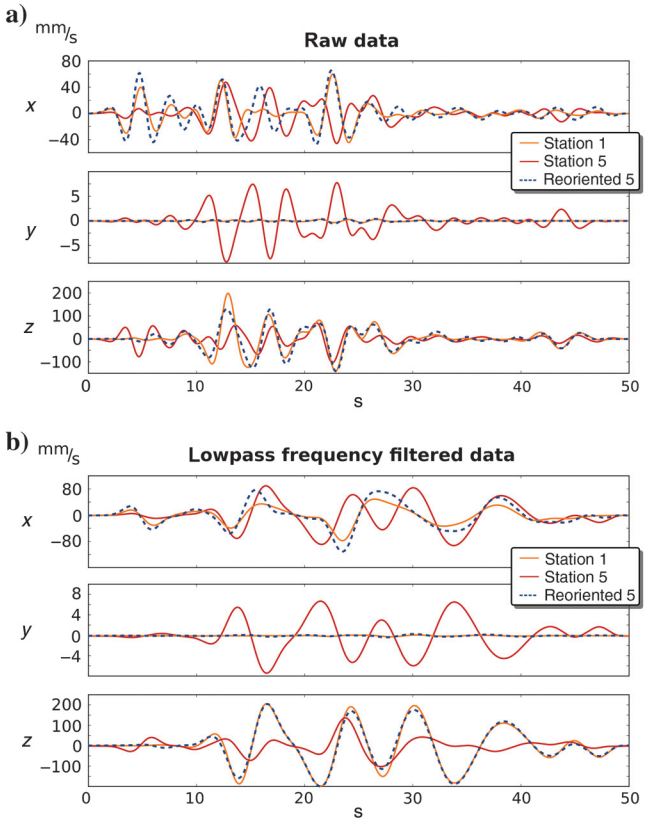

Figure 5. Example of rotated synthetic data from stations 1 and 5 in the VSP geometry. (a) Original raw data. (b) Low-pass frequency-filtered data. The orientation of station 6 (red) is rotated by −93° about the axis (−48.4, −68.5, 54.5) with respect to station 1 (orange). The estimated time lag of the signal between the stations is 0.02 s. The result from the optimal reorientation of station 5 data is shown in blue (dotted line). The estimation deviates from the correct rotation parameters for both data sets: raw data, 1.5° off in the orientation of the axis and 0.4° in the rotation angle; filtered data, 1.8° off in the orientation of the axis and 1.5° in the rotation angle (see Table 2).

the reorientation. However, even between these very good data sets, we obtain differences in the estimated parameters that can be larger than 1°. We have tested other example data sets and found that occasionally these differences can significantly exceed the uncertainty caused by random noise (>10°).

Two-component data — A comparison with a standard reorientation scheme

The standard approach for the reorientation of three-component sensor time-series data is the reduction to two dimensions. One assumes that the vertical sensor axis is sufficiently close to the true vertical. Then, one can determine the optimal rotation angle around this fixed axis using various techniques.

We compare the quaternion method with this standard approach. For this, we use a setup with six seismometers situated at the surface of a flat topography. Again, we assume a distant source of a seismic signal, as depicted in Figure 6, and generate the respective synthetic data sets. The traces are 50 s long, and the sampling rate is 50 Hz. The data (original and low-pass frequency filtered) are shown in Figure 7. Taking into account the previous results, we choose the low-pass frequency-filtered data set in this section, which we assume reduces the estimation errors systematically.

All sensors but the first one (Sta 1) are rotated about an axis that deviates less than 20% from the vertical. This justifies the commonly applied approximation of a correctly oriented vertical axis. The quaternion approach determines a solution in the full 3D space. To be able to compare it with a grid search for a single rotation angle, we have to confine the rotation axis to the respective vertical sensor axis. To achieve this, we set the vertical component of the data to zero for all stations.

As before, we calculate the reorientation twice: first for noise-free data and second, for data with added noise (10% noise amplitude). For each of these, we compare the result with the classical approach of a grid search over 360° in steps of 1°. Within the process of reorientation, we estimate the arrival time lag Δt between stations by a crosscorrelation. The results are given in Table 3 and show the following:

- The quaternion method results are consistently equal to or better than grid-search results ($\mathrm{Res}_{\mathrm{quat}} \leq \mathrm{Res}_{\mathrm{grid}}$).
- The differences between the quaternion method and the grid-search approach are negligible (<0.1%-point).
- The deviation from true data can be large (Res > 40%), even for only slightly tilted rotation axes.

DISCUSSION

We have introduced the theory for expressing rotations in three dimensions using quaternions. Based on this, we adapted a concept presented in Horn (1987), which allows the optimal reorientation of two rotated three-component data sets. The method is based on data that are sufficiently similar and corrected for respective differences in signal arrival times between sensors. An automated correction for the interstation time lag can be achieved by standard crosscorrelation routines, which can be easily implemented together with the frequency low-pass and the reorientation scheme.

Proof of concept

We have shown that the theoretical concept of this method works on data in an optimized setup: Identical data sets have been rotated about various angle-axis combinations in three dimensions. The rotation parameters have been chosen by using uniformly distributed random numbers. The reorientation of the respective data sets yielded no deviation from the original values. After the addition of noise to the rotated data, the reorientation did not perfectly reproduce the original rotation parameters. The deviations have been estimated from matrices $\mathbf{N}$ and $\bar{\mathbf{N}}$, which are derived from the noise-free and noisy data, respectively. Using equations 21 and 22, we calculated both sets of uncertainties, and this shows that the calculation using eigenvectors and eigenvalues of matrix $\bar{\mathbf{N}}$ yields appropriate limits for the deviations of the reorientation from the original parameters.

The normalized data residual Res between the original and reoriented data is large (≈90%). This is purely caused by the high level of random noise on the data, and the large fraction of low-amplitude samples in the data, for which the noise infers large deviations. The level of Res is independent of the actual rotation geometry.

Three-component data

In the application to a VSP geometry (see Figure 3), the data showed slight variations between the stations. This setup is closer to a real data set. The corner frequency for the low-pass frequency filtering of the data had been set to a very low value. This resulted in

Table 2. Quaternion method reorientation of data in a VSP geometry: Numerical values for the parameters of the forward calculation and the estimated reorientation (raw and frequency low-pass filtered data); $\angle\hat{\rho}$ denotes the deviation from axis $\hat{\rho}$. Angles ϵ, α, $\delta\alpha$, $\angle\hat{\rho}$ are given in degrees.

	Forward rotation			Reorientation (raw data)						Reorientation (low-pass-filtered data)				
Station	$\hat{\boldsymbol{\rho}}$	α	$\angle\hat{\boldsymbol{\rho}}$	α	$\Delta\alpha$	Res	ϵ	$\delta\alpha$	$\angle\hat{\boldsymbol{\rho}}$	α	$\Delta\alpha$	Res	ϵ	$\delta\alpha$
Sta 1	—	—	—	—	—	—	—	—	—	—	—	—	—	—
Sta 2	(59.6, 78.9, 15.3)	−50	0.1	−49.9	0.1	10.2	0.54	0.08	0.5	−50.1	0.1	4.9	1.18	0.30
Sta 3	(1.3, −26.9, 96.3)	36	0.4	35.8	0.2	20.8	1.89	0.17	1.1	35.2	0.8	10.6	1.51	2.00
Sta 4	(6.8, 68.3, 72.7)	−4	13.4	−3.8	0.2	31.6	23.17	0.31	20.7	−4.9	0.9	17.0	8.50	3.30
Sta 5	(−48.4, −68.5, 54.5)	−93	1.0	−94.5	1.5	41.5	2.28	2.18	1.8	−93.4	0.4	20.4	3.40	0.71
Sta 6	(67.5, 71.5, 18.2)	−158	1.4	−156.2	1.8	51.1	0.70	3.28	1.5	−159.6	1.6	26.6	2.03	3.95

a clear deviation from the original data set. We showed that data sets with different signal frequency content can lead to significant deviations between the estimated reorientation parameters (>1°). These can be far larger than the influence of noise. This effect cannot be suppressed by just using a low-pass filter with a very low corner frequency. Therefore, we suggest using the quaternion-based reorientation method with different frequency filters to obtain a robust solution. These are independent processing steps; hence, they can be parallelized to reduce computational time.

The absolute level of Res does not necessarily give information about the quality of the parameter estimation. The errors inferred by the addition of noise to the data add to the errors caused by the deviations from different frequency filters. The increase of uncertainty due to random noise can be estimated as before.

Two-component data and comparison with the grid-search method

Having introduced a new reorientation method, we had to show that it works at least as well as a standard processing method. Therefore, we applied a common approximation by assuming that the tilt of the vertical axes of our sensors against the true vertical is negligible. To justify this assumption, we rotated the original data about axes with tilts of <20% (equivalent <18°). Then, we conducted a grid search over 360° for the optimal rotation angle about the true vertical axis. For an appropriate comparison with the quaternion-based method, we had to ensure that the solution space was confined to the same rotation axis. We achieved this by introducing an artificial vertical zero component to the data. By doing so, all reorientations calculated with the quaternion-based method gave the true vertical as rotation axis. This result does not depend on the presence of noise in the remaining two components. The solution obtained using quaternions is always the optimal rotation with respect to the norm of the deviation of reoriented data from the originally recorded data. Indeed, in all cases, the value of Res is lower than the one for the grid-search result. However, it turns out that the difference between the two deviations is fully negligible: The relative variation is usually <0.1%. The influence of noise in this setup is consistent with the results from the former sections. The Res values for both methods increase by approximately the same amount. One important aspect is that the overall level of Res can vary on a large scale (≈0.1% − 40%), and these variations do not necessarily correlate with the small deviations of the rotation axis from the true vertical. This can be taken as a strong argument against the common grid-search approach analyzed here, and as a motivation to use the full 3D reorientations of sensors in the future.

The comparison between the quaternion-based method and the matrix-based approach, which neglects the third components for the benefit of the fast reorientation in only two dimensions, shows that the resulting rotation angles are consistent: The results of the comparison between these two methods are equivalent within the ranges of uncertainties. The latter are determined from the quaternion-based reorientation in addition to the values of the angles.

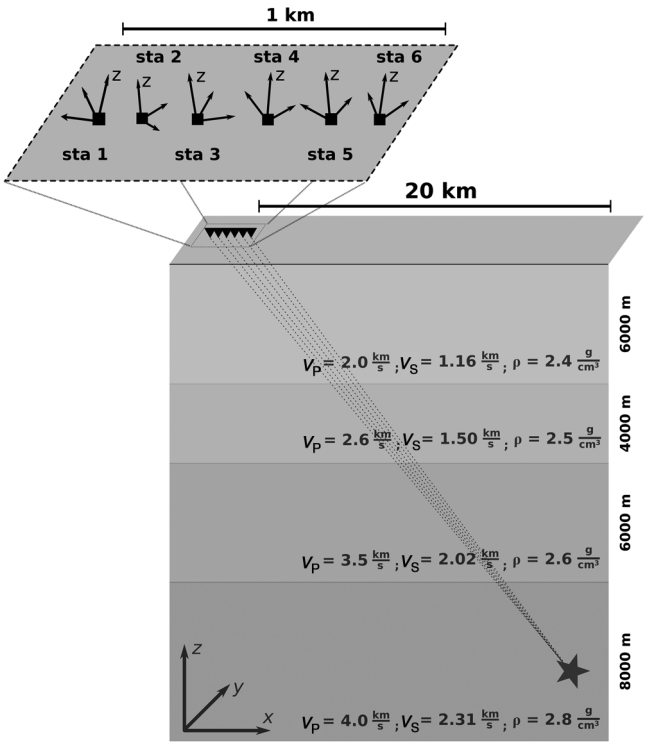

Figure 6. OBS (2D) geometry and earth velocity model for the generation of synthetic seismograms using E3D (Larsen and Grieger, 1998). The (explosive) source location is marked by a star; idealized direct signal raypath sketches are indicated by dotted lines. The model is continued by a half-space underneath the shown layers. The schematic receiver geometry is shown in the enlarged section.

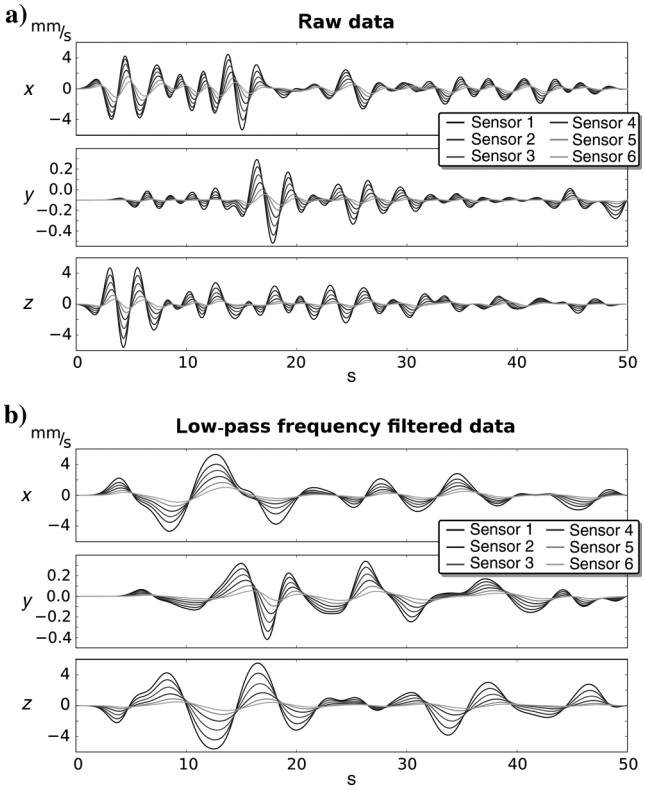

Figure 7. Synthetic data for the OBS geometry shown in Figure 6. The stations are enumerated with increasing distance from the source location. (a) Synthetic data, output from the E3D code. (b) Low-pass frequency-filtered data. The filter is a zero-phase Butterworth low-pass of order 4 with a corner frequency of 0.1 Hz (calculated using ObSpy; Beyreuther et al., 2010).

Table 3. Resulting numerical parameters for the reorientation of data assuming a rotation about the vertical axis: comparison of the quaternion method with a grid search (data noise levels of 0% and 10%). The $\angle\hat{\rho}$ denotes the deviation from the axis $\hat{\rho}$. Angles tilt and α are given in degrees, and Δt is the time shift applied to the data before reorientation.

					Quaternion method				Grid search			
	Original data				No noise		10% noise		No noise		10% noise	
Station	$\hat{\boldsymbol{\rho}}$	Tilt	α	Δt	α	Res	α	Res	α	Res	α	Res
Sta 1	—	—	—	—	—	—	—	—	—	—	—	—
Sta 2	(−5.4, −5.4, 99.7)	4.4	−122	0.08 s	−123.9	14.9	−125.1	51.9	−123.0	14.9	−126.0	51.9
Sta 3	(−23.2, −7.8, 97.0)	14.2	−14	0.22 s	−10.7	14.3	−12.1	53.5	−11.0	14.3	−12.0	53.5
Sta 4	(3.2, 12.1, 99.2)	7.2	−122	0.42 s	−116.3	37.2	−117.3	64.0	−117.0	37.2	−117.0	64.0
Sta 5	(2.9, −8.5, 99.6)	5.2	173	0.70 s	167.5	42.6	165.9	71.7	168.0	42.6	166.0	71.7
Sta 6	(−15.2, −18.0, 97.2)	13.6	111	1.06 s	96.3	49.0	95.6	78.8	97.0	49.0	96.0	78.8

The application to 3D data proves the feasibility of calculating the full 3D reorientation of sensors, including the estimation of uncertainties in rotation angle and axis, respectively. The method is based on the assumption of signals, which are corrected for respective time lags. An automated correction for this interstation time lag can be achieved by standard crosscorrelation routines, which can be easily implemented together with the reorientation scheme.

Remarks

All numerical results shown in this paper have been chosen so that they reflect the overall outcome of a larger number of realizations. We think that the values given are representative for the statistical behavior observed by the authors.

We have used synthetic seismic data for the presented example applications. This was done solely for the convenience of using existing software for their generation and chosen due to the experiences of the authors in this particular field of geophysics. We want to stress that the reorientation as described in this publication is by no means restricted to an application to seismic sensors, but it can be used for all time-series data with two or three orthogonal components. One example for such a data set aside from seismology would be the magnetic field sensors used for magnetotelluric measurements. In magnetotellurics, it is important to know the exact orientation of the sensors for the magnetic flux density, and an appropriate reference station with a known orientation is readily available for most surveys (see Chave and Jones [2012], "Remote referencing").

The intention of this publication was to introduce the theory and proof of concept of the quaternion-based reorientation method. This included analyses with respect to its robustness and potential uncertainties. An application to real data is straightforward, but includes further processing steps, which may depend on the respective data sets. A discussion of such combined processing is not within the intended scope of this work.

CONCLUSIONS

We have presented a method that allows us to find a direct analytical solution for the optimal reorientation of 2D or 3D geophysical time-series data. We used quaternions to express rotations in three dimensions. In addition to the adaptation of this method to a wide class of time-series data sets, we added the application of two theorems from the field of algebra, which allow us to estimate uncertainties of our solution.

For the reorientation of two-component data sets, the quaternion-based method returns the same parameters as a standard approximation. However, the computational effort does not increase by increasing the number of data components and finding rotation parameters in three dimensions. The quaternion-based reorientation yields the optimal parameters as a direct solution; hence, it is more accurate and numerically cheaper than approximative approaches.

The results of the synthetic data examples show that the quaternion-based reorientation works on data from sensors with two or three components. The estimation of rotation parameters is robust under the influence of random noise on the data. To determine an optimal solution, it is vital that the condition $d \ll \lambda$ be satisfied by the data.

We considered the approach of a rotation around a vertical axis in case of tilted sensors. Our numerical values are in accordance with results from a standard grid search for the angle in this case. However, we showed that the deviation between original and rerotated data can be large, even for small offsets of the rotation axis. The short synthetic test data sets used in this work yielded differences up to 40%.

This is a good argument to apply a sensor reorientation using all three spatial dimensions instead of the standard approximative approach. Although numerical solutions from multistep methods can be calculated sufficiently fast, these iterative methods can produce spurious or ambiguous results, for instance, due to a gimbal lock (nonuniqueness of Euler angles). Therefore, we conclude that here as in many other cases, the analytical solution should be preferred over the approximation.

ACKNOWLEDGMENTS

We thank S. Heimann from the Geoforschungszentrum Potsdam for the testing of the numerical code used to calculate the example applications. Furthermore, we deeply appreciate the advice of A. Roberts from the School of Mathematics at the University of Adelaide, who pointed out the theorems required for the estimation of the uncertainties. We thank J. Dellinger, A. Vesnaver, K. Key, and

another anonymous referee for valuable comments and suggestions during the reviewing process. Part of this work has been realized within the research project MINE. The project MINE is part of the research and development program GEOTECHNOLOGIEN, and it is funded by the German Ministry of Education and Research grant of project no. BMBF03G0737A.

REFERENCES

Bauer, F., and C. Fike, 1960, Norms and exclusion theorems: Numerische Mathematik, **2**, 137–141, doi: 10.1007/BF01386217.

Becquey, M., 1990, Three-component sonde orientation in a deviated well: Geophysics, **55**, 1386–1388, doi: 10.1190/1.1442786.

Beyreuther, M., R. Barsch, L. Krischer, T. Megies, Y. Behr, and J. Wassermann, 2010, ObsPy: A python toolbox for seismology: Seismological Research Letters, **81**, 530–533, doi: 10.1785/gssrl.81.3.530.

Brezov, D., C. Mladenova, and I. Mladenov, 2013, New perspective on the gimbal lock problem: AIP Conference Proceedings, **1570**, 367–374, doi: 10.1063/1.4854778.

Cesca, S., A. Şen, and T. Dahm, 2014, Seismicity monitoring by cluster analysis of moment tensors: Geophysical Journal International, **196**, 1813–1826, doi: 10.1093/gji/ggt492.

Chave, A., and A. Jones, (eds.), 2012, The magnetotelluric method: Theory and practice: Cambridge University Press.

Dahm, T., M. Thorwart, E. Flueh, T. Braun, R. Herber, P. Favali, L. Beranzoli, G. D'Anna, F. Frugoni, and G. Smriglio, 2002, Ocean bottom seismometers deployed in Tyrrhenian Sea: Eos, Transactions of the American Geophysical Union, **83**, 309–320

DiSiena, J. P., J. E. Gaiser, and D. Corrigan, 1984, Horizontal components and shear wave analysis of three-component VSP data, *in* M. N. Toksoz, and R. R. Stewart, eds., Vertical seismic profiling, Part B: Advanced concepts: Geophysical Press, 189–204.

Ekström, G., and R. Busby, 2008, Measurements of seismometer orientation at USArray transportable array and backbone stations: Seismological Research Letters, **79**, 554–561, doi: 10.1785/gssrl.79.4.554.

Euler, L., 1775, Formulae generales pro translatione quacunque corporum rigidorum: Novi commentarii Academiae scientiarum imperialis petropolitanae, **20**, 189–207.

Grandi, A., A. Mazzotti, and E. Stucchi, 2007, Multicomponent velocity analysis with quaternions: Geophysical Prospecting, **55**, 761–777, doi: 10.1111/j.1365-2478.2007.00657.x.

Greenhalgh, S., and I. M. Mason, 1995, Orientation of a downhole triaxial geophone: Geophysics, **60**, 1234–1237, doi: 10.1190/1.1443852.

Grigoli, F., S. Cesca, T. Dahm, and L. Krieger, 2012, A complex linear least-squares method to derive relative and absolute orientations of seismic sensors: Geophysical Journal International, **188**, 1243–1254, doi: 10.1111/j.1365-246X.2011.05316.x.

Hamilton, W. R., 1853, Lectures on quaternions, vol. 2: Hodges and Smith.

Hensch, M., 2009, On the interrelation of fluid-induced seismicity and crustal deformation at the Columbo submarine volcano (Aegean Sea, Greece): Ph.D. thesis, University of Hamburg.

Horn, B., 1987, Closed-form solution of absolute orientation using unit quaternions: Journal of the Optical Society of America A, **4**, 629–642, doi: 10.1364/JOSAA.4.000629.

Jurkevics, A., 1988, Polarization analysis of three-component array data: Bulletin of the Seismological Society of America, **78**, 1725–1743.

Kagan, Y., 1991, 3-D rotation of double-couple earthquake sources: Geophysical Journal International, **106**, 709–716, doi: 10.1111/j.1365-246X.1991.tb06343.x.

Key, K., and A. Lockwood, 2010, Determining the orientation of marine CSEM receivers using orthogonal Procrustes rotation analysis: Geophysics, **75**, no. 3, F63–F70, doi: 10.1190/1.3378765.

Landau, L., and E. Lifshitz, 1976, Course of theoretical physics: Mechanics, vol. 3, ed. 3, Butterworth-Heinemann.

Lapilli, C. M., and P. J. Fowler, 2014, Rotation parameters for model building and stable parameter inversion in orthorhombic media: 76th EAGE Conference and Exhibition 2014, Extended Abstracts, doi: 10.3997/2214-4609.20140780.

Larsen, S., and J. Grieger, 1998, Elastic modeling initiative: Part III, 3-D computational modeling: 68th Annual International Meeting, SEG, Expanded Abstracts, 1803–1806.

Li, X., and J. Yuan, 1999, Geophone orientation and coupling in three-component sea-floor data: A case study: Geophysical Prospecting, **47**, 995–1013, doi: 10.1046/j.1365-2478.1999.00160.x.

Menanno, G., and A. Mazzotti, 2012, Deconvolution of multicomponent seismic data by means of quaternions: Theory and preliminary results: Geophysical Prospecting, **60**, 217–238, doi: 10.1111/j.1365-2478.2011.00988.x.

Menanno, G., A. Vesnaver, and M. Jervis, 2013, Borehole receiver orientation using a 3D velocity model: Geophysical Prospecting, **61**, 215–230, doi: 10.1111/j.1365-2478.2012.01106.x.

Michaels, P., 2001, Use of principal component analysis to determine downhole tool orientation and enhance SH-waves: Journal of Environmental and Engineering Geophysics, **6**, 175–183, doi: 10.4133/JEEG6.4.175.

Myer, D., S. Constable, K. Key, M. E. Glinsky, and G. Liu, 2012, Marine CSEM of the Scarborough gas field, Part 1: Experimental design and data uncertainty: Geophysics, **77**, no. 4, E281–E299, doi: 10.1190/geo2011-0380.1.

Nakamura, Y., P. Donoho, P. Roper, and P. McPherson, 1987, Large-offset seismic surveying using ocean-bottom seismographs and air gun: Instrumentation and field technique: Geophysics, **52**, 1601–1611, doi: 10.1190/1.1442277.

Oye, V., and W. Ellsworth, 2005, Orientation of three-component geophones in the San Andreas fault observatory at depth pilot hole, Parkfield, California: Bulletin of the Seismological Society of America, **95**, 751–758, doi: 10.1785/0120040130.

Schrödinger, E., 1926, Quantisierung als Eigenwertproblem: Annalen der Physik, **385**, 437–490, doi: 10.1002/andp.19263851302.

Witten, B., and J. Shragge, 2006, Quaternion-based signal processing: 76th Annual International Meeting, SEG, Expanded Abstracts, 2862–2866.

Yun, X., E. R. Bachmann, and R. B. McGhee, 2008, A simplified quaternion-based algorithm for orientation estimation from earth gravity and magnetic field measurements: IEEE Transactions on Instrumentation and Measurement, **57**, 638–650, doi: 10.1109/TIM.2007.911646.

Zeng, X., and G. McMechan, 2006, Two methods for determining geophone orientations from VSP data: Geophysics, **71**, no. 4, V87–V97, doi: 10.1190/1.2208935.